CHARGE ASYMMETRY AND WEAK INTERACTION EFFECTS IN $e^+e^- \to \mu^+\mu^-$ AND $e^+e^- \to \tau^+\tau^-$

TASSO Collaboration

R. BRANDELIK, W. BRAUNSCHWEIG, K. GATHER, F.J. KIRSCHFINK, K. LÜBELSMEYER, H.-U. MARTYN, G. PEISE, J. RIMKUS, H.G. SANDER, D. SCHMITZ, D. TRINES, W. WALLRAFF
I. Physikalisches Institut der RWTH Aachen, Germany [1]

H. BOERNER, H.M. FISCHER, H. HARTMANN, E. HILGER, W. HILLEN, G. KNOP, L. KÖPKE, H. KOLANOSKI, B. LÖHR, R. WEDEMEYER, N. WERMES, M. WOLLSTADT
Physikalisches Institut der Universität Bonn, Germany [1]

H. BURKHARDT, S. COOPER, D. HEYLAND, H. HULTSCHIG, P. JOOS, W. KOCH, U. KÖTZ [2], H. KOWALSKI [2], A. LADAGE, D. LÜKE, H.L. LYNCH [3], P. MÄTTIG, K.H. MESS, D. NOTZ, J. PYRLIK, D.R. QUARRIE [4], R. RIETHMÜLLER, A. SHAPIRA [5], P. SÖDING, G. WOLF
Deutsches Elektronen-Synchrotron DESY, Hamburg, Germany

R. FOHRMANN, M. HOLDER, H.L. KRASEMANN, P. LEU, D. PANDOULAS, G. POELZ, O. RÖMER, P. SCHMÜSER, B.H. WIIK
II. Institut für Experimentalphysik der Universität Hamburg, Germany [1]

I. AL-AGIL, R. BEUSELINCK, D.M. BINNIE, A.J. CAMPBELL, P.J. DORNAN, D.A. GARBUTT, T.D. JONES, W.G. JONES, S.L. LLOYD, J.K. SEDGBEER, R.A. STERN, S. YARKER [6]
Department of Physics, Imperial College London, England [7]

K.W. BELL, M.G. BOWLER, I.C. BROCK, R.J. CASHMORE, R. CARNEGIE, R. DEVENISH, P. GROSSMANN, J. ILLINGWORTH, M. OGG [8], G.L. SALMON, J. THOMAS, T.R. WYATT, C. YOUNGMAN
Department of Nuclear Physics, Oxford University, England [7]

B. FOSTER, J.C. HART, J. HARVEY, J. PROUDFOOT, D.H. SAXON, P.L. WOODWORTH
Rutherford Appleton Laboratory, Chilton, England [7]

E. DUCHOVNI, Y. EISENBERG, U. KARSHON, G. MIKENBERG, D. REVEL, E. RONAT
Weizmann Institute, Rehovot, Israel [9]

and

T. BARKLOW, J. FREEMAN [10], T. MEYER [11], G. RUDOLPH, E. WICKLUND, SAU LAN WU and G. ZOBERNIG
Department of Physics, University of Wisconsin, Madison, Wisconsin, USA [12]

Received 26 January 1982

For footnotes see next page.

0 031-9163/82/0000–0000/$02.75

We have measured, at an average centre-of-mass energy of 34.22 GeV a forward–backward charge asymmetry in the reaction $e^+e^- \to \mu^+\mu^-$ of value -0.161 ± 0.032. This demonstrates the existence of an axial vector neutral current with coupling strength of $g_a^e g_a^\mu = 0.53 \pm 0.10$. We have also obtained a limit on the vector coupling strength of $g_v^e g_v^\mu < 0.12$. The Weinberg angle is found to be $\sin^2\theta_W = 0.29^{+0.09}_{-0.11}$. From the reaction $e^+e^- \to \tau^+\tau^-$ we have found $g_a^e g_a^\tau < 0.34$, $g_v^e g_v^\tau < 0.55$.

We report on measurements of the reactions $e^+e^- \to \mu^+\mu^-$ and $e^+e^- \to \tau^+\tau^-$ for centre-of-mass energies W in the range 12–14, 22–25 and 30–37 GeV using the TASSO detector at the PETRA e^+e^- storage ring. We have studied these reactions previously [1,2], but the increased data which are now available permit more sensitive tests of QED, and more importantly, a search for weak interaction effects in these reactions.

Contributions from the electromagnetic and weak neutral currents (the latter due to a Z^0 pole) lead to a differential cross section for $\mu^+\mu^-$ or $\tau^+\tau^-$ production of the form [3,4]:

$$d\sigma/d\Omega = (\alpha^2/4W^2)$$

$$\times \{(1 + \cos^2\theta)[1 + 2g_v^2\,\mathrm{Re}(\chi) + (g_v^2 + g_a^2)^2|\chi|^2]$$

$$+ 4\cos\theta\,[g_a^2\,\mathrm{Re}(\chi) + 2g_v^2 g_a^2|\chi|^2]\}\,, \qquad (1)$$

where

$$\chi = (G_F M_Z^2/2\sqrt{2}\pi\alpha)\, W^2/(W^2 - M_Z^2 + iM_Z\Gamma_Z)$$

is the pole term, θ is the scattering angle measured between the incoming positron and the outgoing μ^+ or τ^+, g_v^2 and g_a^2 are respectively the products of the vector and axial-vector coupling constants of the leptons to the neutral current, G_F is the Fermi coupling constant, M_Z and Γ_Z are the Z^0 mass and width. In deriving eq. (1) we have written $g_v^2 = g_v^e g_v^\varrho$ and $g_a^2 = g_a^e g_a^\varrho$ where g^ϱ is the e, μ or τ dimensionless coupling. If lepton universality is assumed $g^\varrho = g^e$. The weak interaction effects grow with W becoming dominant over the pure electromagnetic process for $W \sim M_Z$. At PETRA energies ($W^2 \ll M_Z^2$) possible effects would be a change of the total cross section and a forward–backward charge asymmetry proportional to g_a^2. In the Weinberg–Salam model [3] $g_a = -1/2$ and, using the measured value [5] $\sin^2\theta_W = 0.228$, $g_v = -\frac{1}{2} + 2\sin^2\theta_W = -0.044$. The forward–backward asymmetry

$$A = \frac{N(\theta < \pi/2) - N(\theta > \pi/2)}{N(\theta < \pi/2) + N(\theta > \pi/2)}\,,$$

where N is the number of events in the angular range indicated, would be the most conspicuous effect which to lowest order in G_F (assuming $\Gamma_Z \ll M_Z$) has the form

$$A = -\tfrac{3}{2} g_a^2 \frac{G_F}{2\sqrt{2}\pi\alpha} \frac{W^2}{1 - W^2/M_Z^2}$$

$$= -2.7 \times 10^{-4} g_a^2 \frac{W^2}{1 - W^2/M_Z^2}$$

(W in GeV), which gives at $W = 34$ GeV, $A = -0.09$.

In this letter we present measurements of the total cross sections and the asymmetries in μ pair and τ pair production. The data have been used to obtain values of $g_a^e g_a^\mu$ and $\sin^2\theta_W$, and set limits on $g_a^e g_a^\tau$, $g_v^e g_v^\tau$ and $g_v^e g_v^\tau$ as well as to test QED.

The TASSO detector has been described in detail elsewhere [1,2,6]. In the measurements to be reported here we have relied on the detection of charged particles with the central tracking chambers which cover 87% of 4π. The use of time-of-flight information

[1] Supported by the Bundesministerium für Forschung und Technologie.
[2] On leave at CERN, Geneva, Switzerland.
[3] On leave at UC Santa Barbara, CA, USA.
[4] On leave from the Rutherford Appleton Laboratory, Chilton, England.
[5] Minerva Fellow, on leave from Weizmann Institute, Rehovot, Israel.
[6] Present address: Rutherford Appleton Laboratory, Chilton, England.
[7] Supported by the UK Science and Engineering Research Council.
[8] Present address: Cornell University, Ithaca, NY, USA.
[9] Supported by the Minerva Gesellschaft für Forschung mbH.
[10] Present address: FNAL, Batavia, IL, USA.
[11] Present address: Texas A&M University, TX, USA.
[12] Supported by the US Department of Energy contract WY-76-C-02-0881.

restricted the track acceptance in the polar angle θ to $|\cos\theta| < 0.82$, i.e. 82% of 4π. Muons have been identified using muon chambers [1] and the liquid argon calorimeter [7] each of which covers 49% and together give a combined coverage of 73% of the track acceptance. The τ pairs have been identified by their characteristic charged particle topologies [2]. Cross sections have been determined using the luminosity derived from Bhabha scattering observed in the forward detector and central detector. The luminosity has a systematic uncertainty varying between 3.1 and 5.0%. We first discuss the μ pair production followed by the τ pair production.

The trigger used to detect μ pairs required at least two back-to-back charged tracks coplanar with the beam axis to within 27°. A charged track was identified at the trigger level by requiring connected tracks in the proportional and drift chambers of the central detector and the corresponding time-of-flight counter (ITOF) to have fired.

Events after track reconstruction were required to have:

(a) Two charged tracks each with momentum $p > 0.5\, p_{\text{beam}}$, where p_{beam} is the beam momentum.

(b) The difference between the ITOF measured and predicted time-of-flight for each track to satisfy the condition $-3.0 < (t_{\text{measured}} - t_{\text{predicted}}) < 2.0$ ns.

(c) $|d_0| < 0.4$ cm for each track, where d_0 is the distance of closest approach of the track to the interaction point in the plane perpendicular to the beam axis.

(d) $|z_v| < 4$ cm where z_v is the average displacement of the tracks from the interaction point along the beam axis at their point of closest approach.

(e) An acollinearity angle less than 10° in space.

(f) $|\cos\overline{\theta}| < 0.8$ where $\overline{\theta}$ is the "average" scattering angle defined by

$$\cos\overline{\theta} = \boldsymbol{e}^+ \cdot (\boldsymbol{\mu}^+ - \boldsymbol{\mu}^-)/|\boldsymbol{e}^+| \cdot |\boldsymbol{\mu}^+ - \boldsymbol{\mu}^-|\,,$$

with $\boldsymbol{e}^+$, $\boldsymbol{\mu}^+$, $\boldsymbol{\mu}^-$ being the momentum vectors of the incident positron and the outgoing μ^+ and μ^-, respectively. In the absence of radiative effects and measurement errors the μ^+ and μ^- are collinear and θ [of eq. (1)] = $\overline{\theta}$.

Criteria (a) and (e) are designed to remove τ pair and two-photon scattering ($\gamma\gamma$) events, (b), (c) and (d) to remove cosmic ray events.

Events satisfying these requirements have been identified as μ pairs by demanding one of the tracks to either (i) penetrate the iron absorber and register hits in at least 3 of the 4 layers of the muon chambers or (ii) deposit less than 1.5 GeV equivalent shower energy in a single cluster in the liquid argon calorimeter. [In order to reduce contamination in the lowest energy data, $12 < W < 14$ GeV, both tracks have been identified as muons when only using (ii)]. After this selection we obtained a total of 1764 μ pair events as shown in table 1.

The background in the μ pair sample due to τ pair, cosmic ray, Bhabha and $e^+e^- \to e^+e^-\mu^+\mu^-$ events has been estimated using either Monte Carlo techniques [8] or the data directly. The background from the last two processes is negligible while the τ pairs and cosmic rays lead to small contributions of 1.9 ± 0.6%, 0.4 ± 0.2% for $W \leqslant 25$ GeV and 2.8 ± 0.5%, 0.4 ± 0.2% for $W \geqslant 30$ GeV, respectively. These have been subtracted when calculating the total cross section.

The efficiencies for triggering, reconstructing and selecting the events satisfying criteria (a)–(f) have been calculated using other categories of independently triggered events. These triggers were:

(i) Two large electromagnetic shower energies deposited in opposite hemispheres of the detector.

(ii) Electromagnetic shower energy deposited together with at least one charged track in the central detector.

(iii) An electron or positron tagged in the forward tagging system together with at least one track in the central detector.

Triggers (i) and (ii) select principally Bhabha events and (iii) $\gamma\gamma$ scattering events. With these we have measured independently the efficiencies of all the individual components used for the event detection throughout the running period. The average value of the trigger efficiency was 92.9 ± 0.2% per event, the reconstruction efficiency was 96.6 ± 0.2% and the selection efficiency was 93.9 ± 0.2% per event, leading to an event efficiency of 84.3 ± 0.3%. The variation of the efficiency was less than 1.6% over the range $-0.8 < \cos\theta < 0.8$. The efficiency for muon identification has been evaluated using tracks entering the acceptance of both the muon and the liquid argon calorimeter, and being identified as muons in at least one of the devices. The identification efficiencies for the two detectors were 98.7 ± 0.3% and 96.8 ± 0.7%, respectively.

The geometrical acceptance of the apparatus for μ pairs has been calculated using the Berends–Kleiss Monte Carlo μ pair generator [9]. This has been done separately for the muon chambers and the liquid argon calorimeter so that a comparison could be made. The average acceptance for $|\cos\theta| < 0.8$, including muon identification efficiency, is 73% and nowhere falls below 40% in this range.

In fig. 1 we show for μ pairs, with $W \geqslant 30$ GeV, a plot of the measured normalized reciprocal momentum $R = p_{\text{beam}}/p$ for the forward going muon (R_F) versus that of the backward going (R_B). The sign of R is defined as the charge determined from the track curvature. The events are concentrated at $(R_F, R_B) = (1, -1)$ and $(-1, 1)$ corresponding to the two cases μ^+ forward, μ^- backward and vice versa. The projected R distributions (see fig. 1) have within errors the same mean values $\bar{R}$ and rms resolution σ. For the four categories: forward μ^+, backward μ^+, forward μ^-, backward μ^- these values are:

$\bar{R}_F(\mu^+) = 1.03$, $\sigma = 0.28$; $\bar{R}_B(\mu^+) = 1.02$, $\sigma = 0.29$;

$\bar{R}_F(\mu^-) = -1.00$, $\sigma = 0.30$; $\bar{R}_B(\mu^-) = -1.02$, $\sigma = 0.27$.

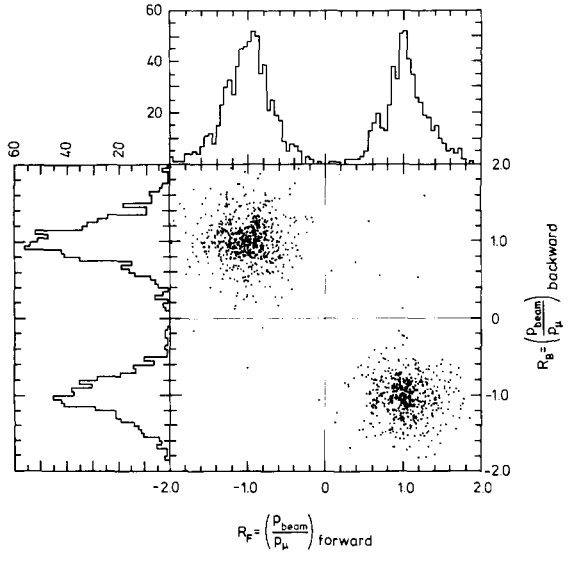

Fig. 1. The normalized reciprocal momentum $R = p_{\text{beam}}/p$ plotted for forward (R_F) and backward (R_B) muons in the reaction $e^+e^- \to \mu^+\mu^-$ at an average $W = 34$ GeV. The sign of R is defined as the charge determined from the track curvature.

These σ values correspond to a momentum resolution of $\sigma_p/p = 0.017\,p$, p in GeV/c. Fig. 1 shows also that for the μ pairs the measurement errors of the two tracks are uncorrelated. The number of events where the same sign of the charge is measured for both muons is for $W \leqslant 25$ GeV: $0\mu^+\mu^+$ and $1\mu^-\mu^-$ out of the 609 μ pairs, for $W \geqslant 30$ GeV: $7\mu^+\mu^+$ and $4\mu^-\mu^-$ out of 1155μ pairs. This leads to a charge confusion probability per track of 0.08% and 0.5%, respectively. The same sign μ pairs have been used for the total cross section but not in the asymmetry measurement.

We have investigated the possibility of a forward–backward bias in the data. In order to introduce an asymmetry such a bias has to lead to a wrong charge sign for both muons, e.g. a $\mu^+\mu^-$ pair changes into $\mu^-\mu^+$ and this has to happen more often, say, if the μ^+ goes forward. Pairs in which both muon tracks change charge will concentrate along the diagonal $R_B = -R_F$ near the origin. Fig. 1 shows that the number of such cases is extremely small and we estimate the probability for both muon tracks to change charge to be less than 0.1%.

To further investigate asymmetry biases we have studied both $\gamma\gamma$ and hadronic annihilation events and find the bias to be <0.01. The test, however, is less significant (with respect to this analysis) since the events do not reflect the μ pair topology.

The differential cross section for μ pair production from lowest order electromagnetic and weak interactions, eq. (1), is of the general form:

$$\mathrm{d}\sigma/\mathrm{d}\Omega = (b_0\alpha^2/4W^2)(1 + b_1\cos\bar{\theta} + b_2\cos^2\bar{\theta})\,, \qquad (2)$$

so that the observed number of events summed over several measurement periods, j, is given by

$$\mathrm{d}n^{\text{obs}}/\mathrm{d}\cos\bar{\theta} = \sum_j (\pi\alpha^2 L_j/2W_j^2)\, b_0 \qquad (3)$$

$$\times (1 + b_1\cos\bar{\theta} + b_2\cos^2\bar{\theta})\, r_j(\cos\bar{\theta})\, f_j(\cos\bar{\theta})\, \eta_j\,,$$

where L_j is the integrated luminosity for that period, $f_j(\cos\bar{\theta})$ is the acceptance, η_j contains all the efficiency factors and $r_j(\cos\bar{\theta})$ is the radiative correction [9] arising from the higher order electromagnetic processes which produce a small asymmetry of $+1.6 \pm 0.5\%$ within $|\cos\bar{\theta}| < 0.8$. We apply the same radiative correction to the electromagnetic and weak process as we would to the pure electromagnetic process.

The coefficients b_1 and b_2 were obtained by maxi-

Table 1
Integrated luminosities, event rates, forward–backward charge asymmetries and results of fits for the reactions $e^+e^- \to \mu^+\mu^-$ and $e^+e^- \to \tau^+\tau^-$.

		W (GeV)		
		12–14	22–25	30–37
$e^+e^- \to \mu^+\mu^-$	average W (GeV)	13.89	22.33	34.22
	L (nb^{-1})	1721	3200	35370
	no. of events	341	268	1155
	b_0	1.05 ± 0.08	1.06 ± 0.09	1.06 ± 0.08
	b_1	−0.05 ± 0.18	−0.37 ± 0.20	−0.45 ± 0.09
	b_2	1.39 ± 0.50	1.23 ± 0.53	1.15 ± 0.26
	$A_{\rm dir}$ ($\lvert\cos\bar{\theta}\rvert < 0.8$)	−0.03 ± 0.05	−0.08 ± 0.06	−0.137 ± 0.029
	$A^{\rm W-S}$ ($\lvert\cos\bar{\theta}\rvert < 0.8$)	−0.013	−0.031	−0.072
	b_1 ($b_2 = 1$)	−0.03 ± 0.16	−0.35 ± 0.19	−0.429 ± 0.085
	A ($\lvert\cos\bar{\theta}\rvert < 1.0$)	−0.01 ± 0.06	−0.13 ± 0.07	−0.161 ± 0.032
	$A^{\rm W-S}$ ($\lvert\cos\bar{\theta}\rvert < 1.0$)	−0.013	−0.036	−0.092
$e^+e^- \to \tau^+\tau^-$	average W (GeV)	13.87	22.33	34.25
	L (nb^{-1})	1759	3248	35806
	no. of events	93	70	262
	b_0	0.98 ± 0.20	1.21 ± 0.23	0.97 ± 0.18
	b_1	0.34 ± 0.32	−0.10 ± 0.61	−0.01 ± 0.21
	b_2	0.34 ± 1.11	3.71 ± 1.99	1.93 ± 0.69
	$A_{\rm dir}$ ($\lvert\cos\bar{\theta}\rvert < 0.8$)	0.09 ± 0.10	−0.07 ± 0.12	−0.01 ± 0.06
	$A^{\rm W-S}$ ($\lvert\cos\bar{\theta}\rvert < 0.8$)	−0.01	−0.03	−0.08
	b_1 ($b_2 = 1$)	0.40 ± 0.33	0.00 ± 0.26	−0.011 ± 0.176
	A ($\lvert\cos\bar{\theta}\rvert < 1.0$)	0.15 ± 0.12	0.00 ± 0.10	−0.004 ± 0.066
	$A^{\rm W-S}$ ($\lvert\cos\bar{\theta}\rvert < 1.0$)	−0.013	−0.035	−0.091

mizing the log likelihood function and their values are summarized in table 1. At all energies b_2 is consistent with the expectation, $b_2 = 1$, and to extract the μ pair cross section via b_0 we use $b_2 = 1$. The total cross sections are shown in fig. 2, as a function of W, and the agreement with QED is excellent ($\chi^2 = 3.1$ for 7 d.f.). The values of b_0 for the three regions are shown in table 1. Any departure from QED can be parametrized in terms of the cutoff parameters $\Lambda_\pm$ defined by

$$\sigma = \sigma_0[1 \mp W^2/(W^2 - \Lambda_\pm^2)]^2 .$$

Fits to the total cross sections yielded $1/\Lambda^2 = (2.17 \pm 2.00) \times 10^{-5}$ GeV^{-2}. The positive and negative bounds on $1/\Lambda^2$ yielded the following 95% confidence limits (CL), $\Lambda_+ > 136$ GeV and $\Lambda_- > 281$ GeV.

Fig. 3a shows the differential cross section (for $W \geqslant 30$ GeV) after corrections have been applied for efficiencies, acceptance and radiative effects. The dashed curve corresponds to the $1 + \cos^2\theta$ form expected from lowest order QED. There is a forward–backward asymmetry, the positive muons emerging preferentially in the backward direction. To quantify this effect we have used two approaches:

(i) The asymmetry has been determined by counting the number of detected events with $0.8 > \cos\bar{\theta} \geqslant 0$ (F) and with $0 > \cos\bar{\theta} \geqslant -0.8$ (B) and forming

$$A^0_{\rm dir}(\lvert\cos\bar{\theta}\rvert < 0.8) = (F - B)/(F + B)$$

and then applying the radiative correction leading to $A_{\rm dir}$. This has the advantage that a detailed knowledge of the acceptance is not necessary to demonstrate the existence of a non-zero asymmetry, since there is no charge dependence in the event acceptance. The values of $A_{\rm dir}$ obtained are shown in table 1.

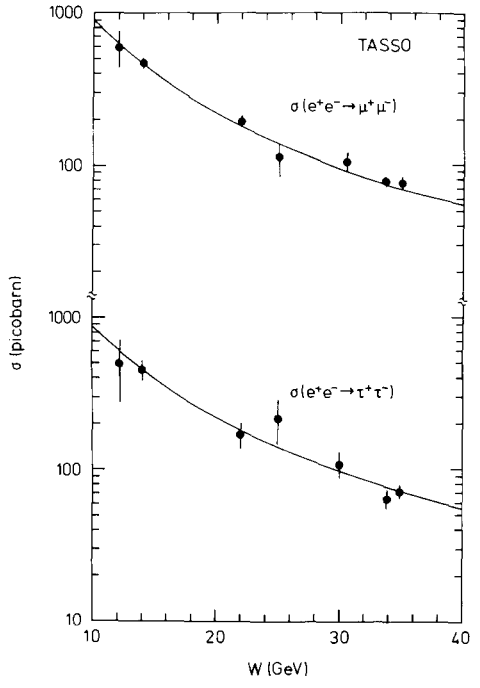

Fig. 2. The total cross sections for the reactions $e^+e^- \to \mu^+\mu^-$ and $e^+e^- \to \tau^+\tau^-$. The curves show the lowest order QED predictions.

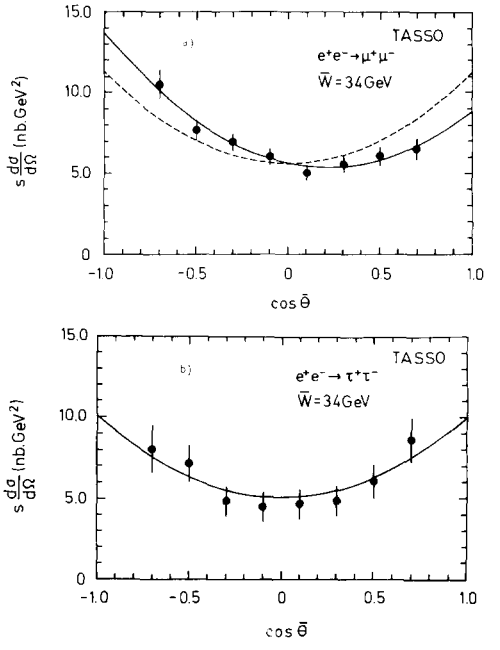

Fig. 3. The differential cross sections at an average $W = 34$ GeV for the reactions (a) $e^+e^- \to \mu^+\mu^-$, (b) $e^+e^- \to \tau^+\tau^-$. The dashed lines have the form $(1 + \cos^2\theta)$ expected from lowest order QED, normalized to the data and the full lines are the results of the fits (see text). For the τ pair data the two curves are indistinguishable and only the full line is shown.

(ii) The angular distribution has been fitted using eq. (3), with $b_2 = 1$, and the asymmetry for the entire angular range obtained from

$$A(|\cos\bar{\theta}| < 1) = \tfrac{3}{8} b_1 .$$

The results of the fits are also shown in fig. 3a and table 1. For energies $W \leqslant 25$ GeV the values of A are consistent with zero, while at $W \geqslant 30$ GeV there is a definite deviation from zero with $A(|\cos\bar{\theta}| < 1) = -0.161 \pm 0.032$. This asymmetry clearly demonstrates the contribution of an axial-vector neutral current. First evidence for this phenomenon was obtained by combining preliminary PETRA results [10]; the JADE measurements have since been published [11]. It is also clear that the results are in broad agreement with the expectations from the Weinberg–Salam model (see table 1).

We have made simultaneous fits to the total cross sections and asymmetries at all energies to determine the parameters g_v^2 and g_a^2 of eq. (1), in the limit that M_Z is infinite. We obtained values of $g_a^2 = 0.53 \pm 0.10$ and $g_v^2 = -0.11 \pm 0.13$ or $g_v^2 < 0.12$ (95% CL). A value of $g_a^2 = 0.44 \pm 0.09$ has been obtained from the asymmetry alone at $\bar{W} = 34$ GeV. Fitting the data with the Weinberg–Salam model with $\sin^2\theta_W$ as the only free parameter we obtained $\sin^2\theta_W = 0.29^{+0.09}_{-0.11}$ ($\chi^2 = 9.4$ for d.f. = 9). This is consistent with the value of [5] $\sin^2\theta_W = 0.228$ derived from lepton scattering experiments which were done at much lower Q^2 values. Finally, we obtained a limit on the size of an additional contribution to the weak neutral current in an extended Weinberg–Salam model [12] where g_v^2 is replaced by $g_v^2 + 4C$. Taking $\sin^2\theta_W = 0.228$ yielded $C = -0.030 \pm 0.030$ or $C < 0.020$ (95% CL).

We now turn to the τ pair production. We have considered events where one τ decay produces three charged particles and the other a single (lone) charged particle. The τ pairs were detected using the triggers in which there were at least two back-to-back charged tracks or four or more charged tracks each with trans-

verse momentum relative to the beam axis, $p_T > 0.32$ GeV/c.

Events after track reconstruction were required to have:

(a) Four reconstructed tracks with total charge zero.

(b) Total charged momentum $\geqslant 5$ GeV/c (6 GeV/c) for $W \leqslant 25$ GeV ($W \geqslant 30$ GeV).

(c) $|d_0| \leqslant 5$ cm and $|z_0| \leqslant 10$ cm for each charged track where z_0 is the distance from the interaction point measured along the beam axis.

(d) An angle of separation of the lone track from all other tracks of $\geqslant 90°$ for $W \leqslant 25$ GeV and $\geqslant 120°$ for $W \geqslant 30$ GeV.

(e) Three charged tracks lying within a cone of 90°, 60° and 45° for $W \leqslant 14$ GeV, $22 \leqslant W \leqslant 25$ GeV and $W \geqslant 30$ GeV, respectively, and the effective mass of the three particles, when considered as pions, to be $\leqslant 2.0$ GeV.

(f) The effective mass $M_{e^+e^-} \geqslant 0.15$ GeV for all oppositely charged pairs of tracks when the particles were assigned electron masses.

(g) The point of intersection of all oppositely charged pairs to be less than 8 cm from the interaction point in the plane perpendicular to the beam axis (i.e. within the beam pipe).

(h) $|\cos\theta_{\text{lone}}| < 0.8$ and $|\cos\theta| < 0.87$ for the other tracks.

(i) $|\cos\bar{\theta}| < 0.8$ where $\bar{\theta}$ is defined as for the μ pairs, using the total momentum vector of the three-track system for one τ and that of the lone track for the other.

Criteria (f) and (g) reduce background from showering Bhabha events, (b), (d) and (e) reduce background from $\gamma\gamma$ scattering and low multiplicity hadronic annihilation events. After this selection we obtained a total sample of 425 τ pair events as shown in table 1.

The background in the τ pair sample due to low multiplicity hadronic annihilation channels and $\gamma\gamma$ scattering has been estimated by Monte Carlo techniques [8,13]. The remaining Bhabha background was estimated from the data using events which failed selection criteria (f) and (g) only. The background from $\gamma\gamma$ induced events is negligible while that from hadronic annihilation is $10.5 \pm 3.4\%$ for $W \leqslant 14$ GeV, $5.5 \pm 3.1\%$ for $22 \leqslant W \leqslant 25$ GeV and $2.7 \pm 1.0\%$ for $W \geqslant 30$ GeV. The corresponding numbers for the background from Bhabha events are $0.5 \pm 0.7\%$, $0.8 \pm 1.1\%$ and $0.8 \pm 0.5\%$.

The efficiencies for triggering, reconstructing and selecting events were calculated using the results of the μ pair efficiency analysis. The only new component is the inefficiency associated with tracks lost because they shared drift cells with other tracks. The number of events lost due to this was estimated by Monte Carlo techniques to be $2.1 \pm 0.1\%$ for $W < 14$ GeV, $7.9 \pm 0.4\%$ for $22 \leqslant W \leqslant 25$ GeV and $14.3 \pm 0.6\%$ for $W \geqslant 30$ GeV.

The acceptance for τ pair events giving a 1 + 3 track topology has been obtained using the Berends–Kleiss generator [9] and using for the product of the τ branching ratios into 1 charged and 3 charged particles [2,14], $B_1 \cdot B_3 = 0.19 \pm 0.03$.

The τ pair events have been analyzed in an analogous manner to the μ pair events [i.e. using eqs. (2), (3)] corrected for efficiencies, acceptance, background and radiative effects. The forward–backward asymmetry arising from the higher order electromagnetic processes [9] is $+0.7 \pm 0.5\%$. The results are summarized in table 1. The total cross sections are shown in fig. 2 and are in excellent agreement with QED ($\chi^2 = 2.9$ for 7 d.f.), the cutoff parameters being $1/\Lambda^2 = 1.3 \pm 4.8 \times 10^{-5}$ GeV^{-2} leading to $\Lambda_+ > 124$ GeV, $\Lambda_- > 104$ GeV (95% CL).

In fig. 3b the angular distribution is shown for $W \geqslant 30$ GeV together with the $1 + \cos^2\theta$ curve expected from QED and the results of the fit with $b_2 = 1$. A direct measurement of the forward–backward asymmetry has been made as well as an extrapolation from b_1. The results are consistent with the Weinberg–Salam model (see table 1). The lower statistics in this channel makes the comparison less significant.

From fits to the τ pair total cross sections and asymmetries at all energies we obtained the following limits on the coupling constants $g_a^2 = g_a^e g_a^\tau < 0.34$ and $g_v^2 = g_v^e g_v^\tau < 0.55$ (95% CL) in the limit that M_Z is infinite.

In summary we have measured the reaction $e^+e^- \to \mu^+\mu^-$ at energies $12 \leqslant W \leqslant 37$ GeV and have observed a significant forward–backward asymmetry of -0.161 ± 0.032 in the highest energy interval ($\bar{W} \doteq 34$ GeV). This is ascribed to the presence of an axial-vector neutral current with a coupling strength $g_a^2 = 0.53 \pm 0.10$. The corresponding vector coupling

strength is $g_V^2 < 0.12$. Assuming the Weinberg–Salam model we obtained $\sin^2\theta_W = 0.29 \pm^{0.09}_{0.11}$. A further contribution to the vector current [12] must have $C < 0.020$. For the reaction $e^+e^- \to \tau^+\tau^-$ we have measured a forward–backward asymmetry at $A = -0.004 \pm 0.066$ for $\bar{W} = 34$ GeV and set limits on the weak coupling constants, $g_a^2 < 0.34, g_V^2 < 0.55$. The μ and τ pair total cross sections are in good agreement with QED leading to cutoff parameters of $\Lambda_+^\mu > 136$ GeV, $\Lambda_-^\mu > 281$ GeV, $\Lambda_+^\tau > 124$ GeV, $\Lambda_-^\tau > 104$ GeV (95% CL).

We gratefully acknowledge the tremendous efforts of the PETRA machine group for the sustained high luminosity running. We thank the technical service groups at DESY and the engineers and technicians at the collaborating institutions. We want to thank Professor F. Berends for help with calculating the radiative corrections. Those of us from abroad wish to thank the DESY directorate for the hospitality extended to us while working at DESY.

References

[1] TASSO Collab., R. Brandelik et al., Phys. Lett. 94B (1980) 259.
[2] TASSO Collab., R. Brandelik et al., Phys. Lett. 92B (1980) 199.
[3] S. Weinberg, Phys. Rev. Lett. 19 (1967) 1264;
A. Salam, Proc. 8th Nobel Symp., ed. N. Svartholm (Almqvist and Wiksell, Stockholm, 1968) p. 367.
[4] R. Budny, Phys. Lett. 55B (1975) 227; Proc. 1975 PEP summer study, LBL-4800/SLAC-190, p. 31.
[5] Particle Data Group, Rev. Mod. Phys. 52 (1980) No. 2, Part II.
[6] TASSO Collab., R. Brandelik et al. Phys. Lett. 83B (1979) 261.
[7] TASSO Collab., R. Brandelik et al., Phys. Lett. 108B (1982) 71.
[8] J. Smith, J.A.M. Vermaseren and G. Grammer Jr., Phys. Rev. D15 (1977) 3280.
[9] F.A. Berends, K.J.F. Gaemers and R. Gastmans, Nucl. Phys. B63 (1973) 381;
F.A. Berends and R. Kleiss, Nucl. Phys. B177 (1981) 237;
F.A. Berends and R. Gastmans, private communication.
[10] J.G. Branson, presented 1981 Intern. Symp. on Lepton and photon interactions at high energies (Bonn, 1981); DESY report 81-073.
[11] JADE Collab., W. Bartel et al., DESY 81-072.
[12] P.Q. Hung and J.J. Sakurai, Nucl. Phys. B143 (1978) 81;
G.J. Gounaris and D. Schildknecht, Univ. Bielefeld report, BI-TP 81/09 (1981);
D. Schildknecht, Univ. Bielefeld report, BI-TP 81/12 (1981).
[13] P. Hoyer, P. Osland, H.E. Sander, T.F. Walsh and P.M. Zerwas, Nucl. Phys. B161 (1979) 349.
[14] J. Kirkby, presented 1979 Intern. Symp. on Lepton and photon interactions at high energies (Fermilab, 1979) p. 107.